http://dx.doi.org/10.14500/aro.12421

Elemental and Organic Matrix Analysis of the Land Snails *Monacha cartusiana* and *Cochlicella barbara* Shells

Hero S. Rahman[1], Dotsha J. Raheem[1†], Fenik Sh. Hussen[2], Hawbash H. Karim[3], Shelan M. Khudhur[4] and Faten A. Chaqmaqchee[3]

[1]Department of Chemistry, College of Science, Salahaddin University-Erbil, Erbil, Kurdistan Region, Iraq

[2]Department of Biology, College of Science, Salahaddin University-Erbil, Erbil, Kurdistan Region, Iraq

[3]Department of Physics, Faculty of Science and Health, Koya University, Koya, Kurdistan Region – F.R. Iraq

[4]Department of Environmental Science and Health, College of Science, Salahaddin University-Erbil, Erbil, Kurdistan Region, Iraq

***Abstract*—In this study, the occurrence of two introduced terrestrial gastropod species: *Monacha cartusiana* (O.F. Müller, 1774) and *Cochlicella barbara* (Linnaeus, 1758), in the Kurdistan Region of Iraq, was investigated. Species identifications were made based on snail morphology. Snail shells were studied to determine their chemical composition and its effect on their success and establishment in the study area. Their organic components (protein and chitin) and inorganic matrix (elements) were analyzed and their correlations were investigated. Elemental analysis was performed using inductively coupled plasma - mass spectrometry and energy dispersive X-ray fluorescence for both species and their surrounding soil. Gravimetric analysis revealed that the main shell component was calcium carbonate ($CaCO_3$) in the form of aragonite, comprising over 96% of the shells' mass. Proteins and carbohydrates accounted for <4% of the shells. Fourier-transform infrared spectroscopy spectral analysis confirmed the presence of chitin in its *β*-allomorph form. Thirty-eight elements were detected. Of which, potassium (K), strontium (Sr), and rhenium (Re) were significantly different between the two species. A highly significant correlation was found between protein and carbohydrates, and $CaCO_3$ indicating the role of the organic matrix in the formation of the mineral component. The survival of the studied species is partly attributed to a considerable overlap in their organic and inorganic chemical characteristics, along with notable differences.**

***Index Terms*—Aragonite, Chitin, Degree of acetylation, Fourier-transform infrared spectroscopy, X-ray fluorescence.**

ARO-The Scientific Journal of Koya University
Vol. XIV, No. 1 (2026), Article ID: ARO.12421. 10 pages
DOI: 10.14500/aro.12421
Received: 11 July 2025; Accepted: 22 February 2026
Regular research paper; Published: 15 May 2026
†Corresponding author's e-mail: dotsha.raheem@su.edu.krd

I. Introduction

The Mollusca constitute a substantial portion of the global fauna and are both the second-largest phylum and one of the most significant groups of creatures on the planet. Gastropod represents the most diverse class within the phylum Mollusca, exhibiting a wide range of habits and forms. Approximately 35,000 terrestrial snails and slugs are acknowledged, with an anticipated 11,000–40,000 cryptic species requiring further identification and characterization. Furthermore, gastropods have successfully colonized the earth and established themselves in arctic and alpine regions as well as deserts and other harsh terrestrial conditions (Schmera and Baur, 2014).

The initial study on the distribution of certain mollusks in Iraq was conducted by Najim (1959), a collection of several freshwater species was made from diverse locations, providing significant insights into their distribution. *Cochlicella barbara* (Linnaeus, 1758) was documented for the 1st time in Iraq, representing an invasive species in this region (Al-Doori, Al-Doori and Al-Juburi, 2018). It was subsequently reported in the Kurdistan region by Bashê and Al-Qassab (2024). In spite of the fact that *Monacha cartusiana* (O.F. Muller, 1774) has been recorded in Baghdad, Iraq, it has not yet been documented in the Kurdistan region (Al-Doori, Al-Doori and Ali, 2023).

The increasing prevalence of invasive species poses a significant threat to global biodiversity and ecosystem function. Understanding the mechanisms that contribute to the establishment and spread of these species is crucial for developing effective management strategies (Gilioli et al., 2017). The snail shell is crucial for their survival. These seemingly solid structures provide physical protection against impacts, can be used to regulate body temperature, and serve as sites for elemental detoxification and sequestration (Kong Yap and Al-Mutairi, 2025; Miller and Denny, 2011). A snail

shell is a mineralized structure primarily composed of calcium carbonate ($CaCO_3$) embedded within an organic matrix of proteins, structural carbohydrates (notably chitin), and other biomolecules. This composition can vary significantly between species and even within populations depending on environmental conditions and physiological adaptations. This variation can influence shell strength, permeability, and resistance to chemical stressors (Jiang et al., 2023).

The organic matrix regulates the construction of the mineral calciferous part over the snail's lifetime. It controls the extent and direction of carbonate crystal deposition. Its ratio may vary due to biological differences and environmental influence, but it is generally a low proportion, making up around 5% in land snails. Understanding the role of the organic matrix and its interplay with the inorganic elemental shell components is important in comprehending the life cycle, habitat preference, and control of these animals (De Paula and Silveira, 2009; Richard and Prezant, 2021; Sundalian, Husein and Putri, 2022). This knowledge is critical for predicting their future spread and potential ecological impacts within Iraqi ecosystems.

This study, therefore, investigates the shell chemical composition of the terrestrial gastropods *C. barbara* and *M. cartusiana* that cohabit the study area. Focusing on proteins, structural carbohydrate (chitin) content, carbonate phase, and general elemental composition. By comparing these parameters, we aim to address the following key points: (i) Differences and similarities in their shell chemical compositions (% mass, $CaCO_3$ polymorphs, protein structure and chitin), (ii) whether the two species exhibit differential elemental accumulation in their shells, and (iii) whether these observed differences influence their survival and ecological fitness within their shared habitat.

II. Materials and Methods

A. Study Area and Sample Collection

The land snails were collected from a residential land about 1 Km east of the 150 M highway in the city of Erbil, north of Iraq (36°11′ 28.28″ N, 44° 0′ 33.08″ E). The site inhabited by both snail species was subjected to salt treatment as an eradication measure at the end of March 2024. This treatment was intended to coincide with the onset of snail emergence from their winter inactivity phase. As more snails became gradually active, they were exposed to the salt and died. Dead snails were collected at intervals of 2–3 days over a 3-week period in April 2024. The samples were transformed to the laboratory where the two species were separated. The shells were cleaned by manually removing dirt and plant debris, followed by washing several times with de-ionized water. They were then allowed to dry at room temperature before being used for further analyses.

B. Diagnosis of Snails

More than 50 live specimens were collected, of which several were cleaned and kept in 70% alcohol for identification. The terrestrial gastropod species were categorized based on shell attributes and other physical traits. Morphological characters were analyzed using a stereoscopic microscope for conchological identification, utilizing several identification keys and studies, including those by Ali and Ramdane (2020), Bashê and Al-Qassab (2024).

C. Soil Samples

To study the extent of elemental uptake and accumulation in the snail shells, it was necessary to apply elemental analysis to the soil from the study area as well. Three soil cores were collected (10 cm^2 surface area) and (10–15 cm depth). The soil samples were air-dried and sieved through a plastic sieve (2 mm^2 aperture size). Equal masses from the samples were combined, homogenized and used in the following elemental analyses.

D. Elemental Analysis Using Inductively Coupled Plasma-Mass Spectrometry (ICP-MS)

The acid digestion was performed following general guidelines described by Li et al. (2015) with modifications. In brief, for acid digestion of snail shells, aliquots of 0.1 g of powdered samples were placed in a Falcon tube with 10 mL of concentrated HNO_3. The tube contents were allowed to stand for 24 h, after which, the mixture was subjected to heating in water bath (70–80°C) for 30 min. The mixture was then filtered and the filtrate was made up to a final volume of 15 mL before subjecting to analysis.

For acid digestion of the soil sample, 5 g of soil was placed in a Falcon tube with 5 mL of concentrated HNO_3. The tube was heated for 5 min in a water bath at (40–50°C), then 6 mL of an acid mixture of 4 mL HF and 2 mL $HClO_4$ was added and heating continued at the same temperature until white fumes emitted. The solution was then allowed to cool down, then 1 mL of HCl was added and the solution was heated again to ensure complete dissolution of the sample. The tube content was finally filtered and the filtrate was made up to 50 mL

Elemental analysis was performed employing an ICP-MS (Agilent 7900 from Agilent Technologies, USA). The instrument was operated with the following parameters: RF generator power of 1200 W, and a resonance frequency of 24 MHz. Argon was employed as the plasma, auxiliary, and nebulizer gas with flow rates optimized at 12.2, 0.8, and 0.8 L/min, respectively. A solid-state charge-coupled device detector was used for ion detection. Each sample was analyzed with an uptake duration of 260 s.

E. Elemental Analysis Using Energy Dispersive X-Ray Fluorescence (EDXRF)

EDXRF was employed to identify and quantify the chemical elements present in the snail shell samples by measuring the emitted energies from the elements upon X-ray excitation (Chaqmaqchee, Baker and Salih, 2017; Meena et al., 2024). This technique allows for multi-elemental analysis with high sensitivity and accuracy. The measurements were performed under vacuum conditions, using a Rigaku NEX CG with RX9, molybdenum (Mo),

copper (Cu) and aluminum (Al) targets. Elemental concentrations were calculated and reported as percentage of the total elemental composition in each sample. The EDXRF Kα X-ray emission lines were used for quantification, where different measuring time were assigned to different targets: 200 s for the Al target and 100 s for RX9, Mo and Cu targets (Ibraheem et al., 2025). This variation in measurement time enhances signal quality on each target's efficiency and energy range to elements being analyzed.

F. Gravimetric Analysis of $CaCO_3$, Proteins, and Chitin Fiber

Demineralization

Powdered shells were demineralized using 1.0 M HCl at a ratio of 1 g to 20 mL. The mixture was stirred at room temperature until emission of CO_2 gas bubbles stopped. The reaction mixture was centrifuged at 4000 rpm for 15 min, the supernatant was discarded then deionized water was used to wash the precipitate until neutral pH was reached. The difference in shell weight before and after demineralization was calculated as the content of $CaCO_3$ (Jatto, Asia and Medjor, 2010).

Deproteinization

The remaining demineralized shell was treated with 1.0 M NaOH at a ratio of 1 g to 20 mL and under reflux at 70°C for 1 h. The reaction mixture was then allowed to stand for 24 h at room temperature before being centrifuged at 4000 rpm. The precipitate was washed several times until neutral pH was reached, then dried in an oven at 70–80°C to constant weight. The difference in weight after this step was calculated as the amount of protein and the residual chitin powder was subjected to further characterization (Sagheer et al., 2009).

G. Fourier-Transform Infrared Spectroscopy (FT-IR) Analysis

FT-IR spectra were collected for the untreated, demineralized, and deproteinized shells in the range of 4000–400 cm^{-1} at a resolution of 4 cm^{-1} and 30 scans using Shimadzu IRAffinity-1 instrument employing an IRsolution software. Sample spectra were acquired by placing a small amount of the samples on the diamond crystal of the attenuated total reflectance compartment. Measurements were performed in triplicate then averaged to minimize variability. The resulting spectra were pre-processed by applying baseline correction, normalization and smoothing. FT-IR spectra were produced using Microsoft Excel 2019 for Windows.

H. Degree of Acetylation (DA%) of the Chitin Chain

FTIR spectroscopy can be used for the calculation of DA% utilizing the ratios of the amide I *ν*C=O to that of the *ν*O-H band (Boukhlifi, 2020) using the following formula:

$$DA\% = \left(\frac{A_{1655}}{A_{3450}} \right) \times 115 \quad (1)$$

Where, *DA%* is the *DA%* of the chitin chain, 1655 and 3450 are stretching vibrations for the C=O and O-H bonds, respectively. These values often vary depending on sample nature and composition, for our samples the band vibrations were 1640 and 3406 cm^{-1}, respectively.

I. Statistical Data Analysis

Statistical analyses were performed using JMP® Pro 18.0.2 statistical software (SAS Institute Inc., Cary, NC, USA). Data are presented as mean±standard error. The level of statistical significance (α) was set at 0.05 for all tests.

Independent samples t-tests were conducted to assess significant differences in the mean values of organic and inorganic components between the two species. Pearson correlation analysis was conducted separately for each snail species to investigate the interrelationships between organic and inorganic components.

III. Results and Discussion

A. Snail Identification

The two snail species were identified from the study area. In *C. barbara* (Linnaeus, 1758), the shell is characterized by a small, narrowly conical and pointed apex, typically brown with distinct white banding. Its dimensions measure between 7.2 and 8.2 mm in height and 4.12–4.62 mm in width. Featuring 7–8 slightly convex whorls separated by shallow sutures, the shell also possesses a very narrow umbilicus. A key observation is that the shell's height is less than twice its width, and its whorls appear relatively flattened. The opaque, whitish shell coloration, frequently adorned with dark bands or blotches, aligns with morphological descriptions provided by Bashê and Al-Qassab (2024) and Khalaf et al. (2020).

M. cartusiana (O.F. Müller, 1774) specimens typically exhibited round shells with 11.4–12.5 mm diameter, comprising 4–5 whorls. The shell exhibits a depressed conical-globular shape, and its umbilicus is partially obscured by the reflected lip. An elliptical aperture features a thickened internal lip. The background shell color is a creamy white, often complemented by an internal white lip that may transition into a reddish line near the aperture, along with occasional faint, transparent pale brown spiral bands. These classifications are consistent with published descriptions by Al-Doori, Al-Doori and Ali (2023), Ali and Ramdane (2020).

B. Gravimetric Analysis of $CaCO_3$, Protein and Chitin Polysaccharide

Gravimetric analysis of inorganic shell matrix components revealed that calcium carbonate is the major component with ratios reaching 98.62% and 98.65% for *M. cartusiana* and *C. barbara*, respectively (Fig. 1). Calcium carbonate is by far the major contributor to a mollusk's shell build-up with reported values ranging from 48% to 98.75% (Sundalian, Husein and Putri, 2022).

The ratio of proteins in, *M. cartusiana,* ranged from (0.72% to 1.29%), while the ratio in *C. barbara* shells ranged from (0.45% to 1.14%) (Fig. 1). Carbohydrates in the shells represented by chitin fiber (will also be referred to as

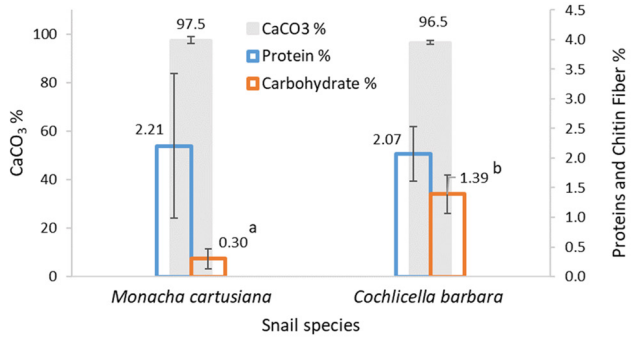

Fig. 1. Percentage shell content of $CaCO_3$ (primary axis), protein and chitin polysaccharide fiber (secondary axis) in *Monacha cartusiana* and *Cochlicella Barbara* snails. Error bars represent standard error. The letters indicate significant differences at $p < 0.05$.

fiber or polysaccharide interchangeably throughout the text) ranged from (0.13% to 0.6%) for *M. cartusiana* and (0.43% to 0.73%) in *C. barbara*. These results are in agreement with previous reports of below 5% content of organic components (De Paula and Silveira, 2009; Jatto, Asia and Medjor, 2010). As depicted in Fig. 1, *M. cartusiana* shells show higher protein levels, whereas *C. barbara* shells demonstrate substantially higher fiber content. However, the differences were found to be insignificant for protein content.

C. FT-IR Analysis of the Mineral and Organic Components

Spectroscopic analysis of the shells revealed the presence of fundamental vibrations typical for the calciferous shell matrix of mollusks (Fig. 2a). The bands at 1445, 855, 700, and 712 cm^{-1}, with assignments detailed in Table I, are characteristic of stretching and bending vibrations of CO_3^{2-} in the aragonite phase of $CaCO_3$ (Vagenas, Gatsouli and Kontoyannis, 2003). The shells of both snails showed similar bands and are therefore predominantly aragonitic.

Absorption bands associated with the organic matrix are partially evident in the spectra of untreated shells, appearing more pronounced in *C. barbara*. However, acid treatment and removal of the carbonate part enhances their visibility. Demineralization of the shells gave the fraction that contained proteins and fiber, shown in Fig. 2b. The main absorptions for the demineralized matrix are amide-specific bands characteristic of proteins and N-acetyl groups of chitin chains. The amide I band is composed of about 80% ν(C=O) and 20% ν(C-N) at 1660–1620 cm^{-1}. The amide II band encompassing about 60% δ(N-H) and 40% ν(C-N) with minor contributions from ν(C-O) and ν(C-C) is spanning lower wavenumbers 1540–1520 cm^{-1}. The amide III band 1240–1220 cm^{-1} is mainly ν(C-N) mixed with δ(N-H). Amide I band showed similar values for both snail species. However slight variations existed between the amide II, III band maxima and $\delta(\text{-}CH_2)$ scissoring and $\delta(\text{-}CH_3)$ side chain vibrations (Table I). A very pronounced difference between the two snail species is the lower ratio of protein glycosylation in *M. cartusiana,* as indicated by the smaller ν(C-O) and weaker, unresolved bands in the glycosidic fingerprint region (Sandt, 2024) in comparison to *C. barbara* (Fig. 2b). This feature is in agreement with the results of the gravimetric analysis of protein and carbohydrate ratio in *M. cartusiana* (Fig. 1).

Deproteinization of the organic matrix leaves behind the chitin fiber (Fig. 2c). Chitin polysaccharide can be found in mollusk shells in two main allomorphs: α- and β-chitin. Each allomorph has a different arrangement of the poly-N-acetylglucosamine chains. The chitin allomorph commonly found in mollusk shells is β-chitin (De Paula and Silveira, 2009). Alpha-chitin can be distinguished from their amide I band which is split into two bands. However. the splitting is less pronounced and the peak may appear broader in the case of β-chitin. Band shape differences were demonstrated by Sagheer et al. (2009), who reported two bands at 1660 and 1620 cm^{-1} for α-chitin attributed to intermolecular hydrogen-bonded CO.HN groups of neighboring chitin chains and intramolecular hydrogen-bonded CO…HO-C(6)H_2, respectively. In the case of β-chitin, a single band was observed at 1656 cm^{-1} for the intramolecular H-bonded CO.HN groups. Both *M. cartusiana* and *C. barbara* demineralized shells showed a single broad band at around 1640 cm^{-1} similar in shape to that reported for the β-allomorph. Close inspection of this band showed that it was a combination of multiple bands at 1658, 1641, 1632, and 1624 cm^{-1}, indicating the sensitivity of this band to different inter- and intramolecular interactions between the amide and hydroxyl moieties of protein and chitin chains. Other features include the amide A (N-H stretching vibration) and amide B bands around 3273 and 3074 cm^{-1}, which are rather broad and not well defined. This feature is in agreement with FTIR spectra of β-chitin rather than α-chitin.

Bands at 798 and 778 cm^{-1} are characteristic of chitin's structure, indicating H-bonding and crystallinity. The 798 cm^{-1} band arises from CH_2 rocking or ring deformation, while the 778 cm^{-1} band is attributed to C-H bending or ring deformation. Further bands at 759, 693, and 647 cm^{-1} confirm the high crystallinity, corresponding to vibrations of N-H, C=O, and O-H bonds, respectively (Agbaje et al., 2021; Sagheer et al., 2009).

D. The DA%

The DA% is the percentage of N-acetyl-D-glucosamine units in the chain, with values above 50% indicating chitin and lower values indicating chitosan. A higher DA% leads to lower solubility, higher crystallinity, and increased strength. It also reduces the number of free amino groups, which impact charge density and metal chelation (Ochi and Babayemi, 2023). The DA% was found to be higher in *M. cartusiana* shell chitin (87.9%) than in *C. barbara* (72.1%), suggesting higher crystallinity and may offer better physical protection for the former (Table II).

E. Elemental Analysis

Elemental analysis was performed for *M. cartusiana* and *C. barbara* shells and their surrounding soil using ICP-MS and EDXRF. The analysis was performed to get insight into bioaccumulation of these elements relative to the soil composition and species-specific variability. Fig. 3a shows

http://dx.doi.org/10.14500/aro.12421

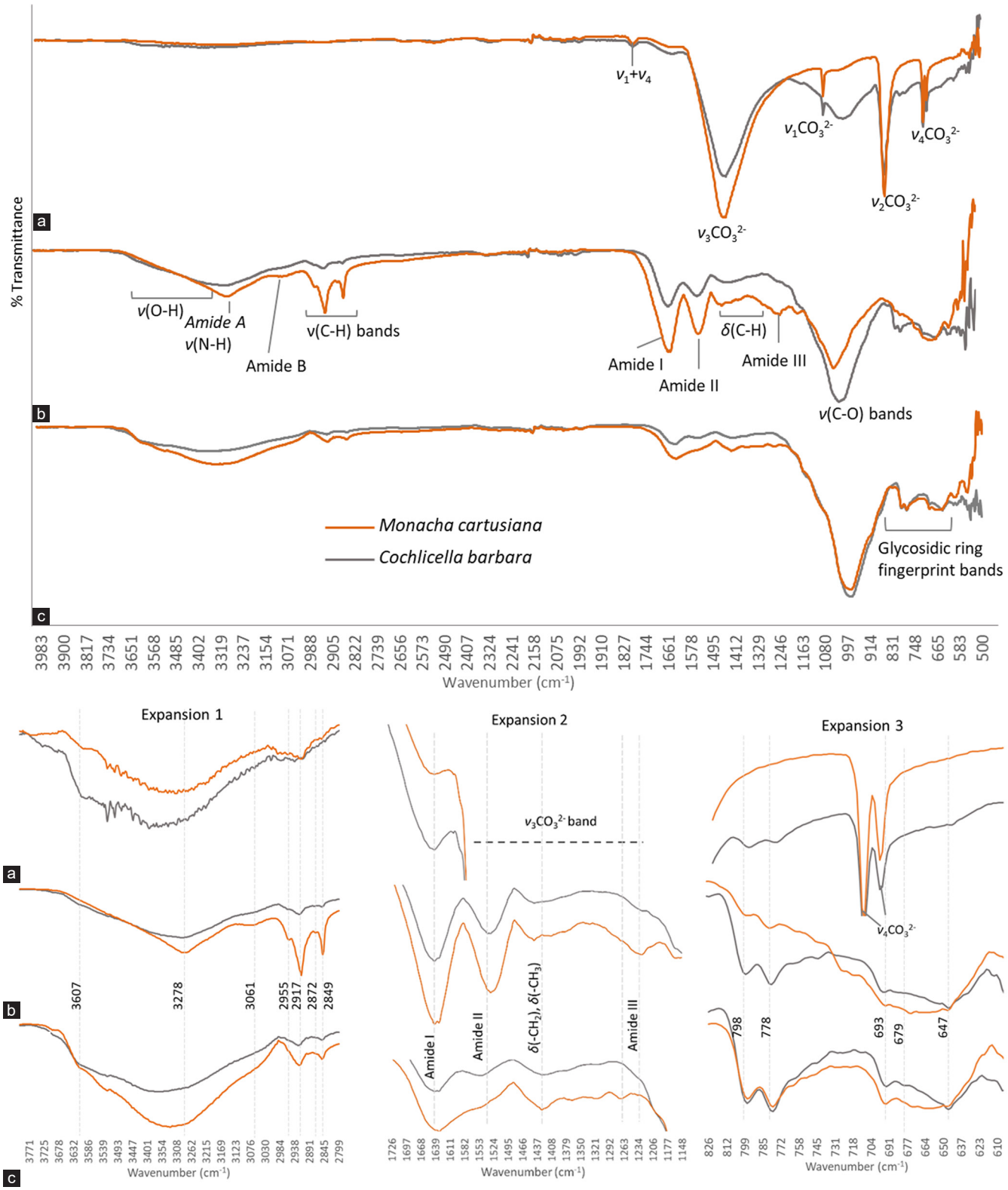

Fig. 2. Top: Fourier-transform infrared spectroscopy spectra of: (a) Untreated shells showing main carbonate bands, (b) demineralized shells showing the main organic matrix bands and (c) deproteinized shells featuring chitin polysaccharide bands of the snails *Monacha cartusiana* and *Cochlicella barbara*. Bottom: Main band regions from the top spectra expanded: Expansion 1 *v*(O-H), *v*(N-H) and *v*(C-H) regions. Expansion 2 includes the amide I-III and aliphatic side chain vibrations. Expansion 3 shows the *δ*(O-H), *δ*(N-H) and glycosidic ring deformation vibrations.

the results from ICP- MS analysis of the shells and soil. Major elements in the soil (above 1000 ppm level) were in descending order: Calcium (Ca), iron (Fe), aluminum (Al), magnesium (Mg), potassium (K), sodium (Na) and titanium (Ti) with concentrations ranging from (44843 ppm) for Ca to (3230 ppm) for Ti.

TABLE I
FOURIER-TRANSFORM INFRARED SPECTROSCOPY FREQUENCY ASSIGNMENTS (CM^{-1}) FOR UNTREATED, DEMINERALIZED AND DEPROTEINIZED SHELLS OF *M. CARTUSIANA* AND *C. BARBARA* SNAILS

Vibrational mode	*M. cartusiana*			*C. barbara*		
	Untreated shells	Demineralized shells	Deproteinized shells	Untreated shells	Demineralized shells	Deproteinized shells
ν(O-H)	3607, several at 3665–3200	3670–3200 br	3614,3526, 3273–3350 br	3607, several at 3665–3200	3670–3200 br	3614,3526, 3273–3350 br
Amide A band (ν(N-H))		3278 br	3273–3350 br		3278 br	3273–3350 br
Amide B band (a Fermi resonance or the first overtone of Amide II band and ν(N-H))		3061	3041		3061	3034
vas(-CH_3)	2961	2955		2956	2956	
vas(-CH_2)	2918	2917	2922	2919, 2925	2918	2922
vs(-CH_3)		2872	2872, 2894		2872	2872, 2894
vs(-CH_2)	2851	2849	2853	2855	2851	2853
($\nu_1 + \nu_4$) CO_3^{2-} combination band	1788			1788		
Amide I band (mainly ν(C=O) inter- and intra-chain H-bonded)	1649, 1638, 1630 w, sh	1658, 1641, 1632, 1624 w, sh	1658, 1640, 1632. 1624 w, sh	1649, 1638, 1630 w, sh	1658, 1641, 1632, 1624 w, sh	1658, 1640, 1632, 1624 w, sh
Amide II band (mainly δ(N-H) mixed with ν(C-N))		1537, 1528, 1523	1557, 1547, 1535		1546, 1536, 1528	1557, 1547, 1535
$\nu_3CO_3^{2-}$asymmetric stretching	1445			1445		
δ(-CH_2) scissoring and δ(-CH_3) symmetric and asymmetric bending of the side chains		1442, 1411, 1370	1427, 1367, 1322		1441, 1413	1427, 1379, 1321
Amide III band (mainly ν(C-N) mixed with δ(N-H))		1237, 1225	1271, 1237 w		1237	1243, 1237 w, sh
ν(C-O) doublet bands of C3-OH of carbohydrate ring		1162	1162 sh, 1150	1163	1162, 1150	1163 sh, 1150
$\nu_1CO_3^{2-}$symmetric stretching	1082			1082		
ν(C-O-H)	1077	1076		1077	1076	
δ(C-O-H), ν(C-O), ν(C-C) skeletal vibration		1074	1069		1076	1070
ν(C-O) of C6-OH of carbohydrate ring	1031	1027	1023	1030	1027	1023
ν(C-O), $\delta\rho$(CH_3)	979 w, sh	979 sh	982 sh	980 sh	979 sh	972 sh
$\delta\rho$(CH_2)	909 w	911 w	910 w	909 w	912 w	910 w
δ(C-O-C) glycosidic linkage deformation $\delta\rho$(C-H)		872 w, sh	873 w, sh		880 w, sh	875 w, sh
$\nu_2CO_3^{2-}$ out-of-plane bending	843, 855			843, 855		
ρ(-CH_2) or ring deformation		798	798	790	797	797
δ(C-H) or ring deformation		779	778	777	778	778
Amide V γ(N-H) of glucosamine		759	762		759	759
$\nu_4CO_3^{2-}$ in-plane bending	700, 712			700, 712		
Amide IV band (δ(C=O) of glucosamine)		693	693		693	693
γ(O-H) of glucosamine		647	646	647	647	646

br: Broad, sh: Shoulder, w: Weak, ν: Stretching, vs: Symmetrical stretching, vas: Asymmetrical stretching, δ: Bending, ρ: Rocking, γ: Out-of-plane bending, amide (I - V): Specific stretching and bending vibrations associated with amide groups of either protein or polysaccharide, ν1 - ν4: Normal modes of stretching and bending vibrations associated with the carbonate group of $CaCO_3$ of the shell matrix. Peak assignments were based on comparison with reported values by (Agbaje et al., 2021; Kumirska et al., 2010; Sagheer et al., 2009; Sandt, 2024; Vagenas, Gatsouli and Kontoyannis, 2003). *M. cartusiana*: *Monacha cartusiana*, *C. barbara*: *Cochlicella barbara*

TABLE II
DEGREE OF ACETYLATION (DA%) FOR *M. CARTUSIANA AND C. BARBARA* SHELL CHITIN CALCULATED APPLYING EQ. 1

Literature band values (cm^{-1})	*M. Cartusiana*			*C. barbara*		
	Measured band values (cm^{-1})	Normalized absorbance	DA%	Measured band values (cm^{-1})	Normalized absorbance	DA%
1655	1640	0.017721	87.9	1640	0.010719	72.1
3450	3406	0.023177		3406	0.017088	

DA%: Degree of acetylation%, *M. Cartusiana*: *Monacha cartusiana*, *C. barbara*: *Cochlicella barbara*

The shells' content parallels the soil's composition for the first five elements. Element ratios were substantially different between the two species, with only Ca and Na reaching above the 1000 ppm level in *C. barbara*. The results were in agreement with (Jatto, Asia and Medjor, 2010), but the quantities varied in comparison to (Potortì et al., 2024). These findings align with previous reports regarding the type of the main elements in snail shells. However, the literature also highlights significant quantitative variability, even among studies of the same species (Badran et al., 2017). This suggests that both taxonomic identity and environmental conditions play a critical role in shell elemental composition.

Calcium showed an overwhelming dominance, which is expected, as shells were over 96.5% composed of $CaCO_3$ (Fig. 1). While *M. cartusiana* showed higher Ca content, the differences were insignificant. The shells' content of Ca was over (5) times their ratio in the soil indicating the active uptake of this element.

http://dx.doi.org/10.14500/aro.12421

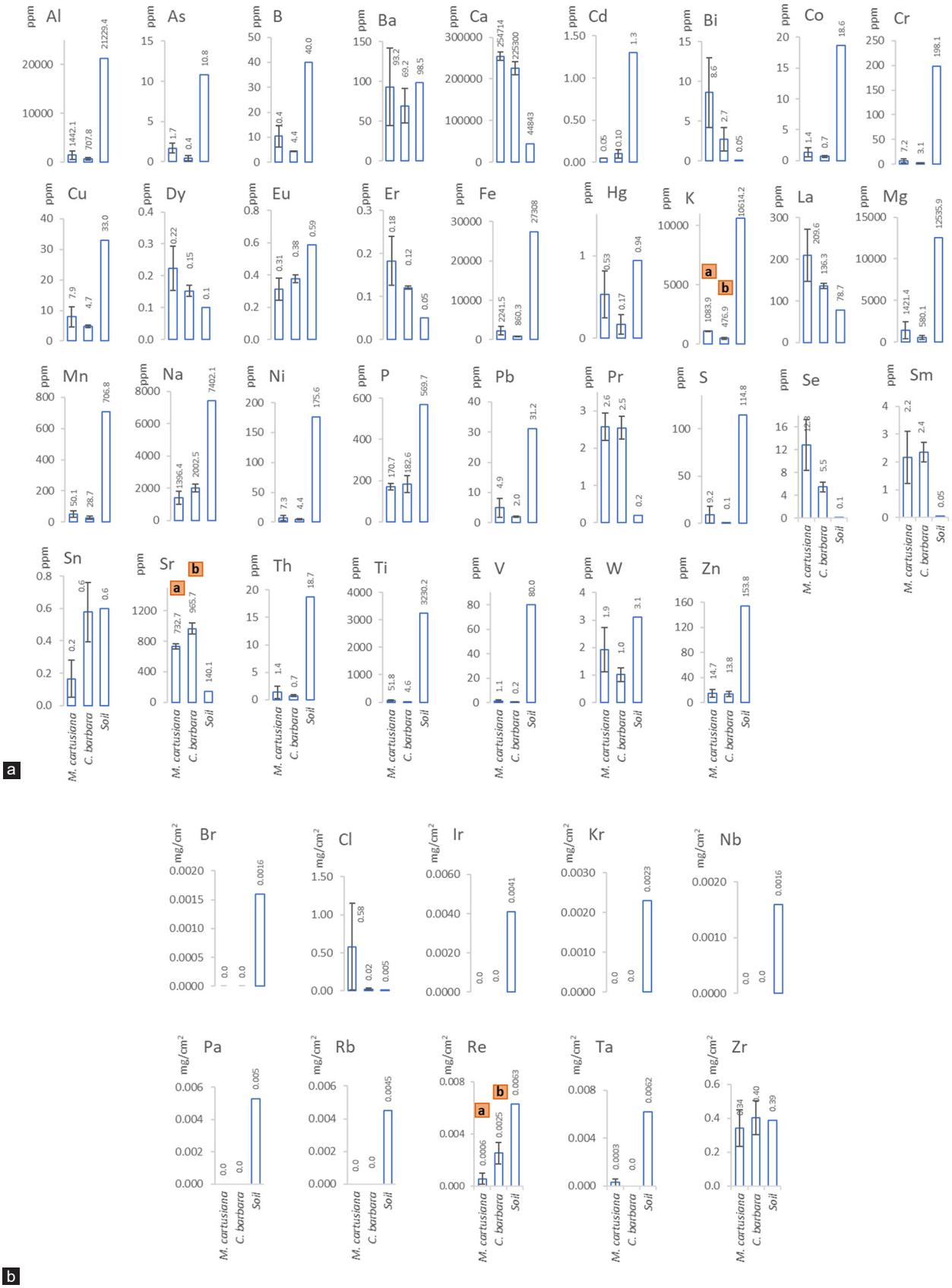

Fig. 3. Elemental content of *Monacha cartusiana*, *Cochlicella barbara* shells and soil from (a) inductively coupled plasma - mass spectrometry and (b) Energy dispersive X-ray fluorescence analysis. The letters a and b indicate significant differences at $p < 0.05$.

M. cartusiana shells showed higher levels of Fe, Al, Mg, and K, with K being the only element showing a significant difference. Sodium was detected in both the snails and the soil, with the high soil concentration likely reflecting the previous NaCl treatment at the sampling site. While pre-cautions were taken to ensure the results accurately reflected the actual Na content, trace residues from the salt treatment at the sampling site may have influenced the final concentrations. Titanium accumulation was noticeably lower in the shells than other major soil elements, which aligns with the findings of Tardugno et al. (2023).

Some elements were found in the shells in concentrations exceeding that in the soil. These included: Barium (Ba), Ca, mercury (Hg), strontium (Sr), and zirconium (Zr), indicating the snail's tendency to actively accumulate those elements.

Elemental accumulation in snails is affected by factors, such as the period of exposure to the pollutant and its concentration in food and the environment. An element's fate in the snail's body is the collective result of absorption, transmission, storage, and integration. Elemental concentration is governed by two main factors in general: Variation related to the snail's biology and environmental factors, with the former having the dominating affect (Baroudi et al., 2020).

A general consensus exists regarding the elemental correlation with the environment (Baroudi et al., 2020). However, the particulars of this correlation can vary. Zhao, Schöne and Mertz-Kraus. (2017) found that Ba, Mg, manganese (Mn), and Sr levels in freshwater *Corbicula fluminea* correlated positively to their environmental concentrations and negatively to temperature. However, findings from Poulain et al. (2015) did not fully support this, which means that species-specific variation can greatly affect their elemental make up. Therefore, further controlled studies would be required to understand uptake and storage extent of different elements in both soft tissues and shells of either of *M. cartusiana* or *C. barbara*.

Elements found in the soil, but not in the shells, included the bromine (Br), the noble gases krypton (Kr) and radon (Rn), the alkali metal rubidium (Rb), and heavy metals niobium (Nb) and palladium (Pa) (Fig. 3b).

The toxic elements aluminum (Al), arsenic (As), cadmium (Cd), chromium (Cr), Hg, and lead (Pb) were found in shells of both snail species. *M. cartusiana* contained higher levels of As, Cr, Hg and Pb. While *C. barbara* shell was higher in Cd. These results are consistent with previous studies demonstrating the rapid bioaccumulation of these metals by land snails from either dietary or soil sources, as well as their adverse physiological effects (Gimbert et al., 2016). A key observation is the high level of Hg in both shells relative to the soil. Mercury has a tendency to bind with biomolecules containing sulfhydryl group, such as the amino acid cysteine and therefore accumulates in parallel with sulfur (Rupa et al., 2023). This explains the reason that *M. cartusiana* contained both high Hg and S.

A significant negative correlation was observed between protein and $CaCO_3$ concentrations in *M. cartusiana*. In contrast, *C. barbara* exhibited a significant intercorrelation among protein, chitin, and $CaCO_3$ (Table III), consistent with the findings of Richard and Prezant (2021). The organic components also correlated with the elements copper (Cu), europium (Eu), Mg, Mn, phosphorus (P) and Ti. This highlights that species-specific differences greatly impact elemental composition, explaining the variations between the two species despite being exposed to the same environmental factors.

TABLE III
Correlation between Organic (Proteins and Chitin) and Inorganic Shell Components

Chemical component	*Monacha Cartusiana*		*Cochlicella barbara*	
	Protein %	**Chitin %**	**Protein %**	**Chitin %**
Protein %	-	0.992	-	**0.999**
Chitin %	0.992	-	**0.999**	-
$CaCO_3$%	**−0.999**	−0.994	**−0.999**	**−0.999**
Al	−0.709	−0.618	−0.975	−0.980
As	−0.823	−0.749	0.371	0.345
B	−0.598	−0.496	−0.871	−0.884
Bi	0.784	0.703	−0.755	−0.737
Ba	−0.691	−0.597	0.809	0.825
Ca	−0.034	0.086	0.112	0.084
Cl	−0.616	−0.516	0.593	0.615
Co	−0.721	−0.632	−0.781	−0.798
Cr	−0.658	−0.562	−0.957	−0.948
Cu	−0.586	−0.484	**−0.997**	**−0.999**
Dy	−0.739	−0.652	−0.406	−0.430
Eu	0.956	0.913	**−0.999**	**−0.998**
Er	−0.579	−0.476	−0.581	−0.603
Fe	−0.717	−0.627	−0.896	−0.908
Hg	−0.913	−0.857	0.422	0.398
K	−0.218	−0.098	−0.906	−0.917
La	−0.571	−0.467	−0.411	−0.436
Mg	−0.673	−0.578	**−0.999**	**−0.998**
Mn	−0.828	−0.754	**−0.999**	**−0.999**
Na	−0.553	−0.448	0.884	0.871
Ni	−0.716	−0.626	−0.954	−0.945
P	−0.990	−0.965	**−0.999**	**−1**
Pb	−0.729	−0.641	0.759	0.740
Pr	0.779	0.698	−0.015	−0.043
Re	−0.437	−0.542	−0.601	−0.623
S	−0.613	−0.513	0.422	0.398
Se	−0.563	−0.459	−0.375	−0.401
Sm	0.771	0.689	0.406	0.381
Sn	−0.616	−0.516	−0.891	−0.90
Sr	0.250	0.365	0.652	0.631
Th	−0.577	−0.474	0.802	0.818
Ti	−0.698	−0.606	**−0.998**	**−0.999**
V	−0.678	−0.584	−0.985	−0.990
W	−0.261	−0.142	−0.841	−0.825
Zn	−0.859	−0.790	−0.979	−0.973
Zr	0.883	0.820	−0.337	−0.363

Bold typeface indicates significant correlations at $p<0.05$

IV. Conclusion

Applying various analytical techniques, including chemical gravimetric analysis, FTIR spectroscopy, ICP-MS, and EDXRF, the organic and inorganic components of *M. cartusiana* and *C. barbara* snail shells were successfully analyzed. Both species shared key characteristics, such as the aragonite polymorph and *β*-chitin allomorph, which likely

contribute to their survival. However, significant differences were also found, including varying protein concentrations and glycosylation levels. *M. cartusiana* showed a higher degree of chitin acetylation, suggesting a stronger shell and better survival prospects. Disparities in elemental concentrations were also noted, with some elements accumulating at higher levels than in the soil, while others were present only in trace amounts. The presence of toxic metals was also a key finding. The specific mechanisms governing elemental uptake and detoxification remain unclear, highlighting a need for further controlled experiments.

V. Acknowledgments

The authors acknowledge the support and resources provided by Salahaddin University-Erbil and Koya University.

References

Agbaje, O.B.A., Brock, G.A., Zhang, Z., Duru, K.C., Liang, Y., George, S.C., and Holmer, L.E., 2021. Biomacromolecules in recent phosphate-shelled brachiopods: Identification and characterization of chitin matrix. *Journal of Materials Science*, 56(36), pp.19884-19898.

Al-Doori, N.L., Al-Doori, M.L., and Ali, R.F., 2023. A classification and the life cycle of snail *Monacha cartusiana* (O.F. Müller, 1774) in Iraq/Baghdad. *Ibn AL-Haitham Journal for Pure and Applied Sciences*, 36(4), pp.1-6.

Al-Doori, N.L., Al-Doori, M.L., and Al-Juburi, H.Q., 2018. A first record and developmental stages of an exotic species *Cochlicella barbara* (Linnaeus, 1758) (Gastropoda-Cochicellidae) in Iraq Baghdad. *Journal of Global Pharma Technology*, 10, pp.104-107.

Ali, R., and Ramdane, R., 2020. Taxonomic key as a simple tool for identifying and determining the abundant terrestrial snails in Egyptian fields (Gastropoda, Pulmonata: Succineidae, Geomitridae, Helicidae, Hygromiidae). *Egyptian Academic Journal of Biological Sciences, B. Zoology*, 12(2), pp.173-203.

Badran, G.B.A., El-Maghraby, L.M.M., El-Massry, S.A.A., and Doheim, M.A., 2017. Biochemial characterstics for snails hemolymph of *Eobania vermiculata* and *Monacha cartusiana* in Egypt. *Zagazig Journal of Agricultural Research*, 44(4), pp.1421-1427.

Baroudi, F., Al Alam, J., Fajloun, Z., and Millet, M., 2020. Snail as sentinel organism for monitoring the environmental pollution; a review. *Ecological Indicators*, 113, p.106240.

Bashê, S.K., and Al-Qassab, S.E., 2024. Morphological and molecular identification of some terrestrial snails: First report. *ZANCO Journal of Pure and Applied Sciences*, 36(1), pp.94-104.

Boukhlifi, F., 2020. Quantitative analysis by IR: Determination of chitin/chitosan DD. In: Khan, M., Do Nascimento, G.M., and El-Azazy, M., Eds. *Modern Spectroscopic Techniques and Applications.* IntechOpen, London, UK, pp.107-131.

Chaqmaqchee, F.A.I., Baker, A.G., and Salih, N.F., 2017. Comparison of various plastics wastes using X-ray fluorescence. *American Journal of Materials Synthesis and Processing,* 5(2), pp.24-27.

De Paula, S.M., and Silveira, M., 2009. Studies on molluscan shells: Contributions from microscopic and analytical methods. *Micron*, 40(7), pp.669-690.

Gilioli, G., Schrader, G., Carlsson, N., Van Donk, E., Van Leeuwen, C.H.A., Martín, P.R., Pasquali, S., Vilà, M., and Vos, S., 2017. Environmental risk assessment for invasive alien species: A case study of apple snails affecting ecosystem services in Europe. *Environmental Impact Assessment Review*, 65, pp.1-11.

Gimbert, F., Perrier, F., Caire, A.L., and De Vaufleury, A., 2016. Mercury toxicity to terrestrial snails in a partial life cycle experiment. *Environmental Science and Pollution Research*, 23(4), pp.3165-3175.

Ibraheem, F.H., Mahmoud, H.E., Saleh, D.I., Smail, J.M., Karim, H.H., and Chaqmaqchee, F.A., 2025. Extraction of nickel oxide from spent catalyst for environmentally safe disposal. *ARO-The Scientific Journal Of Koya University*, 13(1), pp.22-26.

Jatto, O.E., Asia, I.O., and Medjor, W.E., 2010. Proximate and mineral composition of different species of snail shell. *The Pacific Journal of Science and Technology*, 11(1), pp.416-419.

Jiang, C., Storey, K.B., Yang, H., and Sun, L., 2023. Aestivation in nature: Physiological strategies and evolutionary adaptations in hypometabolic states. *International Journal of Molecular Sciences,* 24(18), p.14093.

Khalaf, M.Z., Tareq, A.M., Nahar, F.H., Salman, A.H., and Hamza, B.H.A., 2020. Some aspects of banded conical snail *Cochlicella barbara*: Linnaeus, 1758 (Gastropoda: Cochlicellidae). *Biochemical and Cellular Archives*, 20(1), pp.1479-1484.

Kong Yap, C., and Al-Mutairi, K.A., 2025. Cadmium bioaccumulation and detoxification mechanisms in *Pomacea insularum*: Implications for biomonitoring in freshwater ecosystems. *Frontiers in Environmental Science*, 13, p.1548453.

Kumirska, J., Czerwicka, M., Kaczyński, Z., Bychowska, A., Brzozowski, K., Thöming, J., and Stepnowski, P., 2010. Application of spectroscopic methods for structural analysis of chitin and chitosan. *Marine Drugs,* 8(5), pp.1567-1636.

Li, Y.M., Zhou, X.Y., Yang, J., Sun, Y.X., and Liao, S.Q., 2015. Comparison of three mixed acid digestion methods for the accurate determination of heavy metal concentration in contaminated soil. In: Zhang, J., Ed. *Proceedings of the Environmental Protection and Sustainable Ecological Development, EPSED 2014.* 1st ed. CRC Press, pp.9-14.

Meena, B.I., Karim, H.H., Aziz, Kurdistan F., Chaqmaqchee, F.A., Kokhasmail, D.M., and Hussein, K.N., 2024. Structural characterization of salts using X-ray fluorescence technique: Experiments on samples collected from Kurdistan region of Iraq. *Aro-the Scientific Journal of Koya University*, 12(1), pp.1-7.

Miller, L.P., and Denny, M.W., 2011. Importance of behavior and morphological traits for controlling body temperature in littorinid snails. *The Biological Bulletin*, 220(3), pp.209-223.

Najim, A., 1959. Notes on the distribution of some molluscs in Iraq. *Journal of Molluscan Studies*, 4, p.159.

Ochi, D.O., and Babayemi, A.K., 2023. The physico-chemical properties and sorption potentials of snail shell particulates, chitin, chitosan, and oxalic acid modified chitosan from *Achatina fulica* shell. *European Journal of Sustainable Development Research*, 7(4), p.em0232.

Potortì, A.G., Messina, L., Licata, P., Gugliandolo, E., Santini, A., and Di Bella, G., 2024. Snail shell waste threat to sustainability and circular economy: Novel application in food industries. *Sustainability*, 16(2), p.706.

Poulain, C., Gillikin, D.P., Thébault, J., Munaron, J.M., Bohn, M., Robert, R., Paulet, Y.M., and Lorrain, A., 2015. An evaluation of Mg/Ca, Sr/Ca, and Ba/Ca ratios as environmental proxies in aragonite bivalve shells. *Chemical Geology*, 396, pp.42-50.

Richard, S.R., and Prezant, R.S., 2021. Size related differences in organic and mineral components of Molluscan shell. *American Malcological Bulletin*, 38(2), pp.23-33.

Rupa, S.A., Patwary, M.A.M., Matin, M.M., Ghann, W.E., Uddin, J., and Kazi, M., 2023. Interaction of mercury species with proteins: Towards possible mechanism of mercurial toxicology. *Toxicology Research*, 12(3), pp.355-368.

Sagheer, F.A.A., Al-Sughayer, M.A., Muslim, S., and Elsabee, M.Z., 2009. Extraction and characterization of chitin and chitosan from marine sources in Arabian Gulf. *Carbohydrate Polymers*, 77(2), pp.410-419.

Sandt, C., 2024. Identification and classification of proteins by FTIR microspectroscopy. A proof of concept. *Biochimica et Biophysica Acta (BBA) - General Subjects*, 1868(10), p.130688.

Schmera, D., and Baur, B., 2014. Gastropod communities in alpine grasslands are characterized by high beta diversity. *Community Ecology*, 15(2), pp.246-255.

Sundalian, M., Husein, S.G., and Putri, N.K.D., 2022. Review: Analysis and benefit of shells content of freshwater and land snails from gastropods class. *Biointerface Research in Applied Chemistry,* 12(1), pp.508-517.

Tardugno, R., Virga, A., Nava, V., Mannino, F., Salvo, A., Monaco, F., Giorgianni, M., and Cicero, N., 2023. Toxic and potentially toxic mineral elements of edible gastropods land snails (Mediterranean escargot). *Toxics*, 11(4), p.317.

Vagenas, N.V., Gatsouli, A., and Kontoyannis, C.G., 2003. Quantitative analysis of synthetic calcium carbonate polymorphs using FT-IR spectroscopy. *Talanta*, 59(4), pp.831-836.

Zhao, L., Schöne, B.R., and Mertz-Kraus, R., 2017. Controls on strontium and barium incorporation into freshwater bivalve shells (*Corbicula fluminea*). *Palaeogeography, Palaeoclimatology, Palaeoecology*, 465, pp.386-394.